Xinzhe Lan, Xu Jiang, Yonghui Song, Xingpeng Jing and Xiangdong Xing*

# The effect of activation temperature on structure and properties of blue coke-based activated carbon by $CO_2$ activation

https://doi.org/10.1515/gps-2019-0054
Received December 04, 2018; accepted July 02, 2019.

**Abstract:** Blue coke-based activated carbon (BAC) was prepared via $CO_2$ activation with disused blue coke powder as raw materials at high temperature. The factor of activation temperature was intensively studied. The properties of sample were characterized by $N_2$ adsorption-desorption techniques, scanning electron microscopy (SEM) and Fourier transform infrared (FTIR), and the activation mechanism was also proposed. The results showed that, with the increase of temperature, the yield of BAC decreased, while the iodine adsorption increased first and then decreased. The $N_2$ adsorption-desorption isotherms revealed that the BAC had both micropores and mesopores, and the optimal temperature of porosity development was at 900-1000°C. When the activation temperature reached 1000°C, the maximum Brunauer-Emmett-Teller (BET) specific surface area and pore volume of BAC were 636.91 $m^2 \cdot g^{-1}$ and 0.3627 $cm^3 \cdot g^{-1}$, respectively. The FTIR results indicated that BAC surface contained large amounts of surface functional groups such as hydroxyl, ester, carboxyl, and so on. The content of them decreased with the increase of temperature. Mechanism analysis shows that radial hole-making function happen first then transverd hole-enlarging function as the temperature increases, for the formation of large amount of microporous, the radial activation was the main controlling process.

**Keywords:** blue coke powder; activated carbon; activation temperature; $CO_2$ activation

**List of Abbreviations:**
ad – air-dry basis
$M_{ad}$ – moisture
$A_{ad}$ – ash content
$V_{ad}$ – volatiles
$FC_{ad}$ – fixed carbon
$C_{ad}$ – carbon
$O_{ad}$ – oxygen (by difference)
$H_{ad}$ – hydrogen
$N_{ad}$ – nitrogen
$S_{t,ad}$ – total sulfur
*$FC_{ad} = 100\%-(V_{ad}+A_{ad}+M_{ad})$
*$O_{ad} = 100\%-(C_{ad}+H_{ad}+N_{ad}+S_{ad}+A_{ad}+M_{ad})$
Y – yield
$S_{BET}$ – specific surface area
$S_{micro}$ – microporous specific surface area
$V_{total}$ – pore volume
$V_{micro}$ – microporous pore volume
$d_{ave}$ – average pore diameter

## 1 Introduction

The solid carbon material blue coke is prepared by medium and low temperature dry distillation with Jurassic nonstick coal and high volatile bituminous coal. These raw materials are widespread in the Shaan-Gan-Ning-Meng-Jin Region of Northwestern China [1]. In these areas, blue coke plays an important role in the coal chemical industry, because of its high fixed-carbon content, specific resistance, chemical activity, low ash content, sulfur content, phosphorus content, and volatility. Blue coke is commonly used in industries like calcium carbide, ferroalloy, ferrosilicon and silicon carbide, even as a substitute of metallurgical coke in some field [2].

* **Corresponding author: Xiangdong Xing,** School of Metallurgical Engineering, Xi'an University of Architecture and Technology, Shaanxi Province Metallurgical Engineering and Technology Research Centre, Xi'an 710055, P.R. China,
e-mail: xaxingxiangdong@163.com
**Xinzhe Lan, Yonghui Song,** School of Metallurgical Engineering, Xi'an University of Architecture and Technology, Shaanxi Province Metallurgical Engineering and Technology Research Centre, Xi'an 710055, P.R. China
**Xu Jiang,** School of Metallurgical Engineering, Xi'an University of Architecture and Technology, Shaanxi Province Metallurgical Engineering and Technology Research Centre, Xi'an 710055, P.R. China; Research Institute of Energy and Chemical Industry, Xianyang Vocational Technical College, Xianyang, 712000, P.R. China
**Xingpeng Jing,** Institute of Coalbed Methane Development and Engineering, Xi'an Research Institute Company Limited, China Coal Technology and Engineering Group, Xi'an, 710054, P.R. China

During blue coke production, transportation, and storage, the powder byproduct with the grain size < 6 mm is inevitably generated, which has very low utilization and causes serious environmental challenges [1]. Statistics show that nearly one million tons of blue coke powder is being produced every year in Yulin Area, which seriously affects the sustainable development of the blue coke industry [3]. Finding clean and efficient processing and utilization technology of blue coke powder has great significance for the sustainable development of the blue coke industry.

One of the effective strategies to treat this challenge is producing the blue coke-based activated carbon (BAC), where the blue coke powder is transformed into the activated carbon using certain techniques. As the blue coke is easy to obtain, and activated carbon is widely used in daily life and industrial fields, this strategy shows promising prospect for application. Although the BAC was successfully obtained by activation with chemical agent and steam from our previous study, the chemical activation method has some drawbacks including high pollution, strong corrosiveness, the remainder activating reagent on the surfaces of BAC cannot be removed completely [4], the main problem of steam activation method is high energy consumption and low microporosity. So the industrialization promotion of BAC preparation technology needs more efforts.

Carbon dioxide is a commonly used and an effective activator for the activation techniques of activated carbon (AC), since it is clean, cheap, easy to obtain, and facile to control. A type of microporous AC was prepared from Pinang frond using $CO_2$ as the activation agent [5]. The specific surface area and the pore volume of the products is 958.23 $m^2/g$ and 0.5469 mL/g, which has 87.6% adsorption rate of Remazol Brilliant Blue R (RBBR). Carbon dioxide activation for the super-activated carbon [6] yields a product with a 3500 $m^2/g$ specific surface area and a 1.84 $cm^3/g$ pore volume at 1100°C. Ruidong Zhao et al. [7] studied the effect that the marketed coconut shell activated carbon reactivation by $CO_2$ had on pore structures. The micropore volume of product increases from 0.21 $cm^3/g$ to 0.27 $cm^3/g$, the specific surface area increases from 627.22 $m^2/g$ to 822.71 $m^2/g$, and there is a 23.77% increase in absorption capacity for the phenol after reactivation. By comparison with other activating reagent, the $CO_2$ activation results in a better microporous structure, a larger micropore volume, and a narrower pore size distribution. Jerzy Choma et al. [8] studied the effects that $CO_2$ and KOH activation had on the pore structure of AC made from Kevlar-derived carbon fibers. The results show that AC activated by $CO_2$ has a more abundant microporous structure and has a better adsorption effect on $CO_2$. The specific surface area and the pore volume is 1240 $m^2/g$ and 0.61 $cm^3/g$, when the reaction is performed at 750°C for 3 h. Min She et al. [9] investigated the micropore morphology of AC via $CO_2$ and $H_3PO_4$ activation with rice husk as the raw material. The results indicate that the AC activated by $CO_2$ has flask shaped micropores and the specific surface area is 563.06 $m^2/g$, which is greater than when activated by $H_3PO_4$. The microporous activated carbon that was prepared by K. Suresh Kumar Reddy et al. [10] through $CO_2$ activation with date palm pits as the raw material had an average pore size of 1.51 nm. However, another AC activated by $H_3PO_4$ has additional mesopores with an average pore size of 2.91 nm. Xiangkun Jian et al. [11] found that the micropore content between 0.5-1.0 nm obtained by $CO_2$ activation are 10% greater than when obtained by steam activation in the same experiment conditions. Similar conclusions have been drawn by Arenas [12] and Alcaniz [13]. Many scholars have studied the main controlling factors of $CO_2$ activation. Mohammad Mazlan et al. [14] suggest that temperature is the main factor of rubber wood sawdust activation via $CO_2$. With the increase of activation temperature, the specific surface area, the pore volume, and the microporosity initially increase and then decrease. The process of $CO_2$ physical activation with a Hawaii nut shell raw material was analyzed using response surface methodology by Song Cheng et al. [15], showing that the activation temperature and the time have the greatest effect on the development of AC micropores. The temperature is shown to be the main control indicator of the activation process [16-18].

Although $CO_2$ is a mature and high quality activation agent, few studies have focused on the activation of disused blue coke powder. In this paper, disused blue coke powder was employed to prepare the BAC with $CO_2$ activation at high temperatures. The activation mechanism was explored by investigating the effect of activation temperature on the pore structure and the surface properties. The obtained results provide fundamental insights into the preparation process of BAC. Our results will also offer guidance in utilizing disused blue coke powder to prepare BAC.

## 2 Materials and methods

### 2.1 Materials

The blue coke powder was provided by Shenmu Sanjiang Coal Chemical Co., Ltd. The industrial and the elemental analyses of the blue coke powder are shown in Table 1.

**Table 1:** Industrial analysis and elemental analysis of the blue coke powder.

| | Industrial analysis | | | | Elemental analysis | | | | |
|---|---|---|---|---|---|---|---|---|---|
| Sample | $M_{ad}$ | $A_{ad}$ | $V_{ad}$ | $FC_{ad}$ | $C_{ad}$ | $O_{ad}$ | $H_{ad}$ | $N_{ad}$ | $S_{t,ad}$ |
| Blue coke powder | 2.15 | 16.77 | 12.07 | 69.01 | 72.88 | 0.32 | 1.06 | 0.88 | 0.61 |

## 2.2 Methods

### 2.2.1 Raw material pre-treatment

The blue coke powder with granularities ranging between 2 mm to 3.2 mm were immersed in 1.0 mol/L hydrochloric acid and sodium hydroxide solution for 12 h respectively. The solid sample was washed with distilled water until the pH was neutral. The material was stored in an airtight package after it was dried at 110°C in a vacuum oven (DZF–6053) for 12 h.

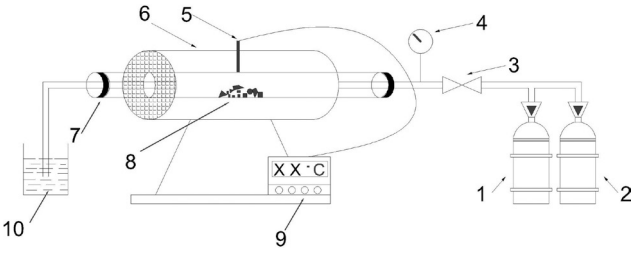


**Figure 1:** $CO_2$ activation device.
1 – $CO_2$ Steel cylinder, 2 – $N_2$ Steel cylinder, 3 – Valve, 4 – Flowmeter, 5 – Thermocouple, 6 – Tubular furnace, 7 – Quartz reactor, 8 – Raw material, 9 – Temperature controller, 10 – NaOH solution.

### 2.2.2 Preparation of BAC

BAC preparation was conducted as follows: 5.0 g of blue coke powder after pre-treatment was placed into a self-made quartz reactor, which was placed into tubular heaters (TCXT–1700) and heated to 600°C, 700°C, 800°C, 900°C, 1000°C, and 1100°C under the protection of nitrogen. When heating to the activation temperature, $CO_2$ was added, instead of $N_2$, under a 200 L/h gas flow rate. After 120 min of activation, adding $CO_2$ was stopped, and the BAC was cooled to room temperature under $N_2$. The resulting materials were termed BAC–600, BAC–700, BAC–800, BAC–900, BAC–1000, and BAC–1100. The experimental device is shown in Figure 1.

### 2.2.3 Characterization of prepared BAC

The yield was calculated from the mass ratio of product to raw material. The iodine number was determined following GB/T 7702.7–2008 (China). The nitrogen adsorption-desorption isotherm was obtained using a fully automatic physical adsorption apparatus (ASAP2420) at 77.35 K. The specific surface area of the BAC was calculated based on the Brunauer-Emmett-Teller (BET) model. The total pore volume and the pore size distribution of the BAC were analyzed via the Barrett-Joyner-Halenda (BJH) method. The micropore volume of the BAC was calculated with the t-plot method. The mesopore volume of the BAC was the difference between the total pore volume and the micropore volume. The microporosity of the BAC was the ratio of micropore volume to the total pore volume. The morphology of the BAC was examined via JSM-6700F scanning electron microscopy (SEM). The surface functional groups of the BAC were identified by IR-Prestige-21 Fourier transform infrared (FTIR) spectroscopy.

# 3 Results and discussion

## 3.1 The iodine adsorption value and the yield of BACs

The effect of the activation temperature on the iodine adsorption value and the yield of BACs are shown in Figure 2. The iodine adsorption value was regarded as an important index for measuring the level of activation, the microporous structure, and the adsorption capacity. The iodine adsorption value of the BACs initially increased between 600-1000°C, and then decreased as the activation temperature increased (Figure 2). When the temperature was higher than 700°C, particularly between 900°C to 1000°C, the iodine adsorption value increased drastically. At 1000°C, the iodine adsorption value reached to maximum, 856.19 mg/g.

The yield represented the loss of raw material in the process of activation, which could reflect the changes of the pores inside the material to some extent. Figure 2 shows that the yield of the BAC decreased gradually as the temperature increased. When the temperature rose from

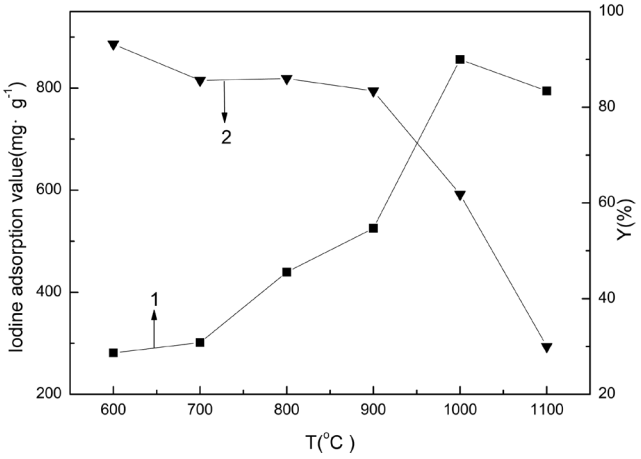


**Figure 2:** The effect that the activation temperature had on the iodine adsorption value and the BAC yield.
1 – Iodine adsorption value and 2 – Yield.

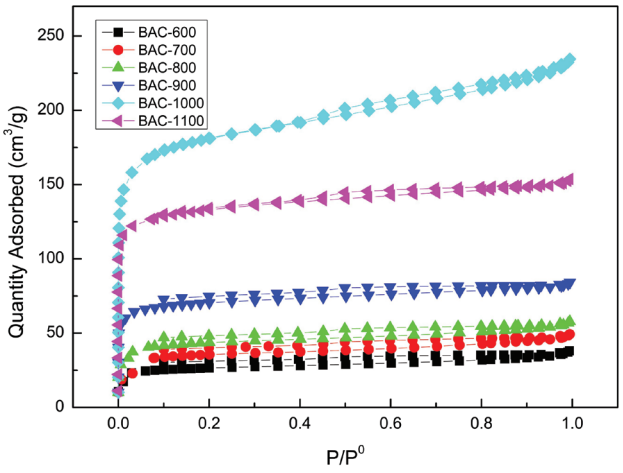


**Figure 3:** $N_2$ adsorption-desorption isotherm of the BACs.

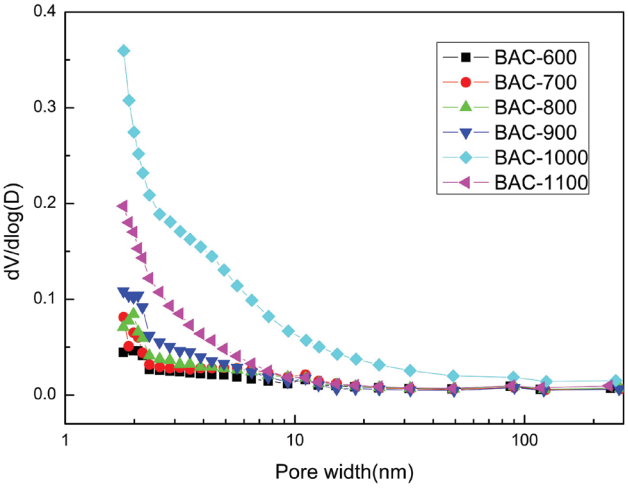


**Figure 4:** Pore size distribution of the BACs.

900°C to 1000°C, and then to 1100°C, the yield decreased from 83.4% to 61.8% and then to 30.0%, respectively. This illustrated that the carbon inside the raw material was continuously lost. The new pores during $CO_2$ activation were constantly generated.

The results of the analysis showed that activation reaction rate of blue coke powder with $CO_2$ was increased dramatically when the temperature was higher than 700°C. The reaction was even more severe when the temperature reached 900°C. At this point, the large amount of pores that were produced caused a sudden drop in yield, which was beneficial for the adsorption. The reduction of the iodine adsorption value when the temperature continued to rise to 1100°C can be attributed the over-activation of the raw materials, which led to a large number of carbon being overreacted and consumed. The entire structure of BAC loosened and a large number of micropores evolved into mesopores or macropores, so the adsorption capacity was weakened.

## 3.2 The pore structures of BACs

The nitrogen adsorption-desorption isotherm of BAC was studied to characterize the porosity texture of carbonaceous adsorbents, and analyzed in to further investigate the effects of the temperature on the specific surface area and the pore structure. The isotherm could provide structure parameters of the adsorbent, which were an important index for measuring the adsorption properties. The nitrogen adsorption-desorption isotherms, the pore size distribution, and the pore structure parameters of the BACs are shown in Figures 3 and 4, and Table 2.

As seen in Figure 3, the isotherms of BACs had a similar tendency, where it shifted upward gradually initially and then downward as the temperature rose, which indicated that the BAC adsorption capacity of $N_2$ increased first and then decreased. The isotherm moved up obviously when the temperature rose from 900°C to 1000°C, which was the optimal temperature range. The adsorption capacity of $N_2$ increased from 83.22 cm³/g to 234.49 cm³/g. When the temperature increased to 1100°C, the isotherm moved down and the adsorption capacity of $N_2$ dropped to 153.74 cm³/g, which were in good agreement with those obtained by the iodine adsorption value analysis.

The results of nitrogen adsorption-desorption isotherms were used to calculate pore structure parameters, which is shown in Figures 2. The BET specific surface area, the microporous specific surface area, and the micropore volume of the BACs initially increased and

**Table 2:** Pore structure parameters of the BACs.

| Sample | $S_{BET}$ ($m^2 \cdot g^{-1}$) | $S_{micro}$ ($m^2 \cdot g^{-1}$) | $V_{total}$ ($cm^3 \cdot g^{-1}$) | $V_{micro}$ ($cm^3 \cdot g^{-1}$) | $V_{micro}/V_{total}$ (%) | $d_{ave}$ (nm) |
|---|---|---|---|---|---|---|
| Blue coke powder | 7.77 | - | 0.025 | 0.002 | 7.62 | 13.05 |
| BAC–600 | 75.50 | 48.22 | 0.059 | 0.029 | 49.38 | 3.119 |
| BAC–700 | 93.59 | 62.30 | 0.076 | 0.039 | 51.52 | 1.469 |
| BAC–800 | 126.60 | 84.99 | 0.089 | 0.049 | 55.06 | 2.822 |
| BAC–900 | 247.44 | 190.50 | 0.130 | 0.084 | 64.52 | 2.104 |
| BAC–1000 | 636.91 | 457.40 | 0.363 | 0.201 | 68.87 | 2.28 |
| BAC–1100 | 503.40 | 407.50 | 0.238 | 0.164 | 55.50 | 1.89 |

then decreased as the activation temperature increased. The BAC with maximum BET specific surface area and pore volume were obtained when the temperature was 1000°C, and the values were 636.91 $m^2/g$ and 0.363 $cm^3/g$ respectively. The pore structure parameters decreased when the temperature rose to 1100°C, indicating that the optimal activation temperature was 1000°C.

As shown in Figure 3, the isotherms belong to combination of type I and IV according to the International Union of Pure and Applied Chemistry (IUPAC) classification. The adsorption capacity increased sharply as $P/P_0 < 0.1$, owing to the greatest adsorption rate at this time. When $P/P_0 > 0.1$, the adsorption capacity remained unchanged, the shape of isotherm change to a horizontal platform, this proofs that the isotherms belongs to the type I according to the IUPAC classification. The van der Waals force caused a significant increase of adsorption potential inside the micropores, due to the adsorption force of pore with a short distance superimposed on each other. The absorption of $N_2$ on BACs surface was a rapid process, which was completed at low relative pressure during a surprisingly short time. The characteristic of the microporous adsorption was present. Meanwhile, when the relative pressure was close to 1, the adsorption capacity of BACs increased slightly, and the isotherm showed a tailing and hysteresis phenomenon, which indicating that the isotherms belongs to the type IV also, and there were some mesopores and macropores inside of the BACs in addition to the micropores. As seen in Table 2, the microporosity of the BACs remained between 49.38% and 68.87%.

The pore size distributions of the BACs calculated by the BJH method is illustrated in Figure 4, where they had different shapes, but similar trends. The maximum peak occurred at BAC–1000, which had the most well-developed pore structure. The pore size peaks of the products were obtained between 1.5 mm to 2.5 mm, which indicated that the vast majority of the pores fell within the micropore and mesopore range. This conclusion confirmed the pore structure parameters and the results from the nitrogen adsorption-desorption isotherms.

## 3.3 The SEM images of BACs

SEM was used to observe the surface physical morphology of materials. The SEM images of BACs are shown in Figure 5. With rising of activation temperature, the morphology of BACs in the front side (Figures 5a-f) and the lateral sides (Figures 5g-l) had obvious differences. The morphologies of front side is observed from axial direction of pores, and the lateral side is observed from radial direction, which perpendicular to the direction of front side. When the temperature reached 600°C, the BAC–600 had very few pores, as seen from both front side (Figure 5a) and lateral sides (Figure 5g), which showed that the activation rate was relatively low at this temperature. As the activation temperature increased, the roughness and the defects gradually began to emerge in the surface of the material, which caused slit-shaped pores. The development of the fiber's structure in the BACs was shown from the lateral sides of the products. The formation of pores and the rising of temperatures would help the $CO_2$ diffuse into the inner the material, which further accelerated the process of $CO_2$ activation and the pore formation.

When the activation temperature rose to 1000°C, the front of BAC–1000 morphology (Figure 5e) showed many circular pores with different apertures in material surface, which formed into a honeycomb cavernous structure. The fiber vascular structure of BAC–1000 also advanced in lateral the sides of the morphology (Figure 5k), which signified that the well-developed pore structure had been formed.

The pore wall of the BAC–1100 had been destroyed as the temperature increased, and the additional macropores are formed from the collapse of mesopores and micropores.

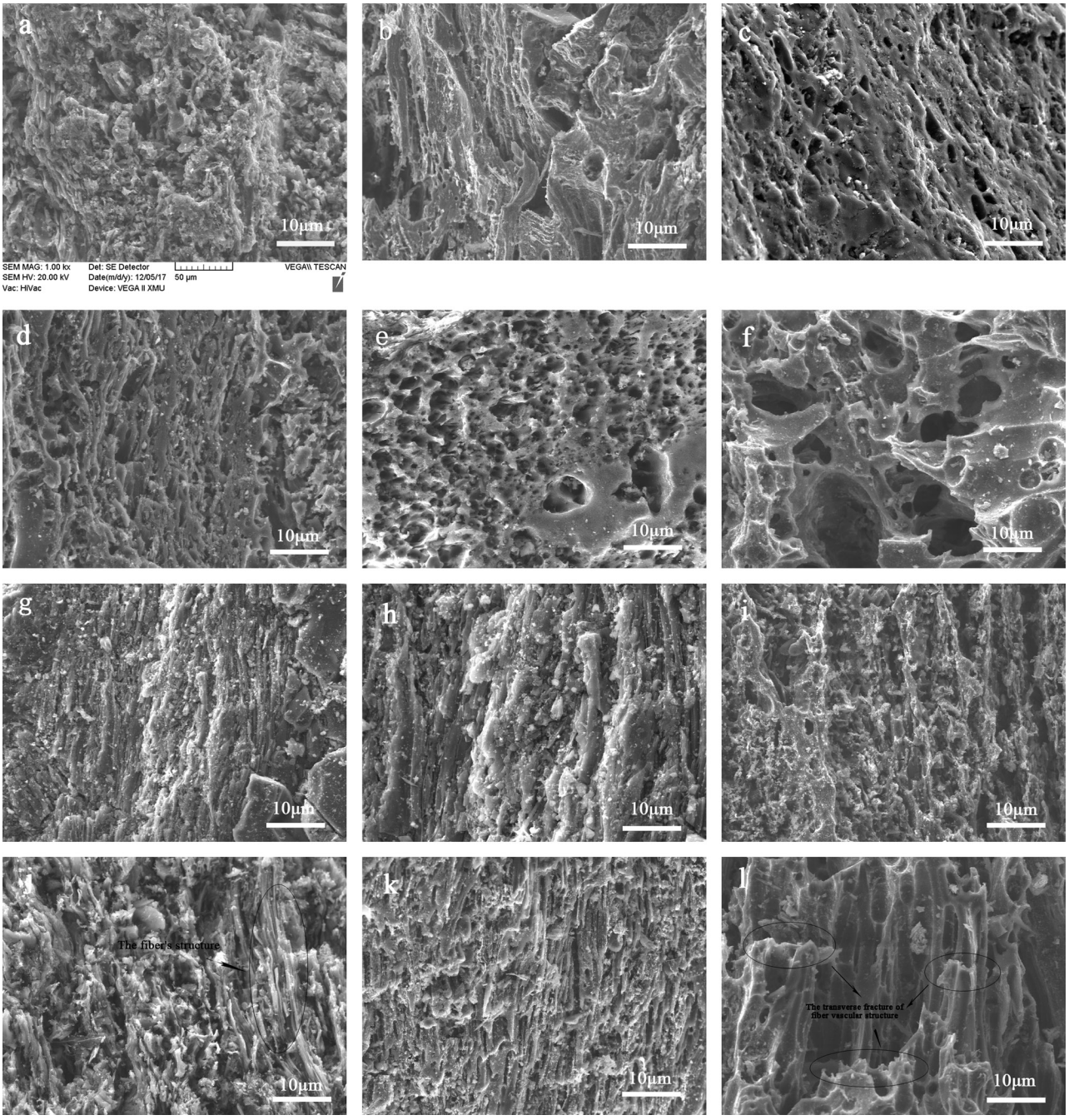


**Figure 5:** SEM images of BACs: (a,g) BAC-600, (b,h) BAC-700, (c,i) BAC-800, (d,g) BAC-900, (e,k) BAC-1000, (f,l) BAC-1100.

As seen from the lateral sides of the morphology (Figure 5l), the pores of BAC–1100 had a transverse fracture, the original fiber vascular structure was destroyed. These changes of pore morphology was proof that the BAC–1100 was over-activated, which was in good agreement with the experimental result of the adsorption isotherms and the pore structure parameters that were analyzed previously. There were some irregular solid particles that adhered to the surface of the BACs, these particles were the ash of the raw material that did not react with the $CO_2$ in the high temperature.

## 3.4 The surface functional group of BACs

The surface functional groups on the BACs were analyzed by FTIR, and the results are shown in Figure 6. The broad absorption bands at 3650-3250 $cm^{-1}$ were due to

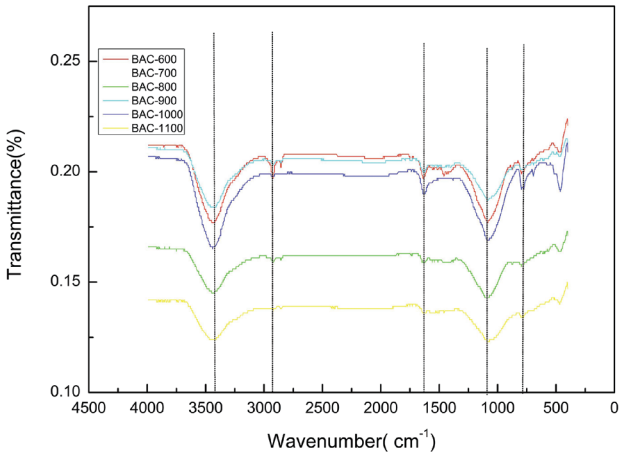


**Figure 6:** FTIR spectra of the BACs.

the stretching vibration of the hydroxyl (O–H) [19] or the water molecule adsorbed by the BACs [20]. The weak absorption peaks at 2920-2840 $cm^{-1}$ were attributable to the C–H stretching vibration of the asymmetric aliphatic hydrocarbons, which showed that the BACs contained some $-CH_2$ and $-CH_3$ groups. The weak absorption bands at 1600-1400 $cm^{-1}$ were indexed to the stretching vibration of C=O and C=C, or by the in-plane bending vibration of N–H, which indicated that the BACs contained some carboxylic acid, fatty ketone, or amino groups functional groups. The absorption peaks at 1300-1000 $cm^{-1}$ were attributed to the C–O stretching vibrations, which are resulted from the hydroxyl, ester, and ether functional groups on the surface of the BACs [21]. The characteristic absorption peaks of the BACs were similar, although the intensity of absorption peak gradually decreased as the temperature increased. When the activation temperature exceeded 1000°C the absorption bands at 2920-2840 $cm^{-1}$ and 1600-1400 $cm^{-1}$ were no longer observed. This was because the side chains of partial functional groups in the surface of the raw material broke and separated from the carbon skeleton by the $CO_2$ activation at high treatment temperatures, which led to the decreased content of the surface functional groups. The activation temperature had an obvious influence on the content of the surface functional groups.

## 3.5 Activation mechanism analysis

The essence of the $CO_2$ activation was a process of partial gasification reactions between C and $CO_2$, which exhibited an endothermic reaction. The reaction formula is described as follows (Reaction 1):

$$CO_2 + C \rightarrow 2CO \qquad \Delta H = 173.3\ KJ/mol \tag{1}$$

The reaction mechanism is described in Reactions 2-5:

$$C^* + CO_2 \rightarrow C^*(CO_2) \tag{2}$$

$$C^*(CO_2) \rightleftharpoons C^*(O) + CO \tag{3}$$

$$C^*(O) \rightleftharpoons CO \tag{4}$$

$$CO + C^*(O) \rightleftharpoons C^*(CO_2) \tag{5}$$

where C* is the active point in the blue coke crystallites and ( ) means the atom or molecule in brackets is the adsorption state.

From a microscopic perspective, the activation reaction starts from the activity sites in the surface of raw material, which exhibited a high affinity. These activate sites were primarily distributed in the end, the section, and the lattice defect of the blue coke microcrystallites [22]. The heat transfer from the outside to the inside as the temperature rise. The detailed activation reaction is described as follows: the $CO_2$ diffused to the active sites and is adsorbed on them at the beginning of the activation reaction. As the temperatures increased, reactions seen in Reactions 3 and 4 occurred. The CO was produced and released because of these two reactions. Partial oxygen atoms were attached to the surface of the blue coke [23], which produced CO with blue coke, or formed $CO_2$ with CO as Reaction 5 illustrated. Consumption of CO as seen in Reaction 5 effectively accelerated Reactions 3 and 4, which promoted the activation reaction, resulted in continuous consumption of blue coke.

The macro level analysis revealed that the $CO_2$ activation went through three procedures: hole-throughing, hole-making, and hole-enlargement [24]. The activation process was divided into three stages in different temperature ranges: the initial activation stage (600-900°C), the rapid activation stage (900-1000°C), and the over-activation stage (1000-1100°C). There were two main types of $CO_2$ activation regarding to the pore development at different temperatures: the radial activation and the transverse activation. The variation of pore structure are shown in Figure 7.

When the temperature reached 600°C, the activity sites in the surface of raw material were present only on a small percentage of the specific surface area, so the reaction was slow. With the rise of the activation temperature, the reactivity of the carbon atom on the surface of the blue coke increased, and the diffusion rate of $CO_2$ molecule transport into the blue coke interior sped up. This resulted in the increased reaction rate as the reactive probabilities of $CO_2$ with the carbon atom increased. The activated reaction was mainly in the radial direction rather than transverse direction [25], which resulted in

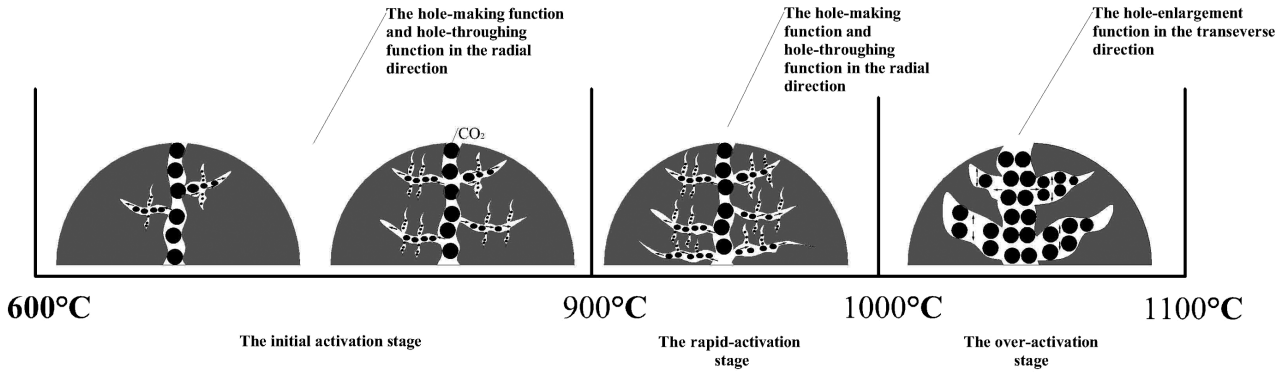


**Figure 7:** The variation of pore structure in $CO_2$ activation.

new micropores forming continuously in the materials. The pore structure parameters also increased at the same time. The radial activation had a lower activation reaction rate, and was a progressive process. In addition, a small number of molten coal tar existed in the blue coke, which was decomposed into gaseous hydrocarbons escaping from the material to remove the blockage in pores.

The reaction rate accelerated rapidly due to the raised activity of the carbon atoms on surface of the raw material when the temperature increased to 1000°C. The carbon atom on the edges and the dislocations of the blue coke powder were reacted and eroded continuously. The activation reaction remained running from outside to inside and the yield dropped significantly. The hole-making function was a result of the radial activation and was dominant in this stage. The through-hole function occurred constantly, which induced the formation of a large number of new micropores and the pore structure parameters of the BACs increased.

The activation reaction was further aggravated when the temperature reached 1100°C, but the radial activation was not obvious, due to the decreased temperature gradients from inside to outside, so the reaction between C and $CO_2$ occurred in the transverse direction. The transverse activation was stronger than the radial activation, which resulted in significant pore wall thinning and increased average pore sizes, suggesting the hole-enlargement function took place. The fibrous vascular structure of the BAC–1100 was burnt out and led to a collapse, where the number of mesopores and macropore rose and the yield decreased sharply. The collapsed carbon in the BAC–1100 would block the pores. This was caused the decline of the pore structure parameters and the iodine adsorption value. Similar conclusions were obtained by Roman et al. [26], who prepared AC from olive stone via $CO_2$ activation.

By mechanism analysis, with the increase of temperature, a large number of micropores were initially produced because of radial activation. The transverse activation then took place, the micropores collapse caused the production of mesopores and macropores. In order to obtain the activated carbon with well-developed microporous structure and a high specific surface area, the radial activation via the control of activation temperature must be paid more attention.

## 4 Conclusions

(1) The activation temperature had a remarkable effect on the pore structure and the adsorption properties of the BACs. As the activation temperature increased, the iodine adsorption value increased first then decreased, and the yield declined continuously.

(2) The activation temperatures between 900°C and 1000°C were the best stages of the activation process. The highest specific surface area and the pore volume were 636.91 $m^2 \cdot g^{-1}$ and 0.363 $cm^3 \cdot g^{-1}$. The $N_2$ adsorption isotherm belonged to the combination of type I and IV according to the IUPAC classification, which indicated that the sample had both a microporous and a mesoporous structure.

(3) The FTIR results indicated that the BACs contained surface functional groups of hydroxyl, ester, ether, and carboxylic acid. The surface functional group content of the BACs decreased gradually as the activation temperature increased, but there were few significant effects on the type of surface functional groups.

(4) The $CO_2$ activation was essentially the partial gasification between C and $CO_2$, which began at the activity sites in the surface of the raw material that exhibited a high affinity. The activation of the radial hole-making function from outside to inside initially occurred, and then the transverse hole-enlargement

function took place. The radial activation was controlled by the activation temperature, which was beneficial for the preparation of the BAC with well-developed micropores and a high specific surface area.

**Acknowledgements:** This project was financially supported by the National Natural Science Foundation of China (51774227) and the Scientific Research Plan Projects of Shaanxi Education Department (No. 17JK1170).

## References

[1] Song Y.H., Ma Q.N., Li X., Zhou J., Tian Y.H., The influence of activation temperature on structure and properties of semi-coke-based activated carbon. Mater. Rev., 2016, 30(1), 34-37.

[2] Tian Y.H., Lan X.Z., Song Y.H., Liu C.B., Zhou J., Preparation and characterization of formed activated carbon from fine blue-coke. Int. J. Energy. Res., 2015, 39, 1800-1806.

[3] Tian Y.H., Lan X.Z., Li L.B., Chen X.Y., Hu T.H., Preparation of activated carbon from blue coke powder and its adsorption properties of Cr(VI). Adv. Mater. Res., 2010, 10, 1347-1351.

[4] Tian Y.H., Lan X.Z., Zhou J., Chen X.Y., Li L.B., Reparation of activated carbon from blue coke powder by microwave radiation and KOH activation. Chem. Eng., 2010, 38(10), 225-228.

[5] Ahmad M.A., Herawan S.G., Yusof A.A., Effect of activation time on the pinang frond based activated carbon for remazol brilliant blue R removal. J. Mech. Eng. Sci., 2014, 12(7), 1085-1093.

[6] Plaza-Recobert M., Trautwein G., Pérez-Cadenas M., Alcañiz-Monge J., Superactivated carbons by $CO_2$ activation of loquat stones. Fuel Process. Technol., 2017, 159, 345-352.

[7] Zhao R.D., Liu F.L., Zheng S.R., Wan H.Q., Xu Z.Y., Adsorption of phenol on $CO_2$-treated activated carbon. Environ. Pollut. Control, 2010, 32(10), 33-36.

[8] Choma J., Osuchowski L., Marszewski M., Dziura A., Jaroniec M., Developing microporosity in kevlar-derived carbon fibers by $CO_2$ activation for $CO_2$ adsorption. J. $CO_2$ Util., 2016, 16, 7-22.

[9] She M., Duan Y.F., Zhu C., Hong Y.G., Zhou Q., Wang S.Q., Experiment study on mercury adsorption performances of rice husk chars activated by $CO_2/H_3PO_4$ and modified by $NH_4Br$. J. Southeast Univ.: Nat. Sci. Ed., 2014, 44(2), 321-327.

[10] Reddy K.S.K., Shoaibi A.A., Srinivasakannan C., A comparison of microstructure and adsorption characteristics of activated carbons by $CO_2$ and $H_3PO_4$ activation from date palm pits. New Carbon Mater., 2012, 27(5), 344-351.

[11] Jian X.K., Liu S.C., Bian Y., Effect of activation medium on microstructure and $CO_2$ adsorption performance of activated carbon. J. Funct. Mater., 2014, 45(1), 1095-1098.

[12] Arenas E., Chejne F., The effect of the activating agent and temperature on the porosity development of physically activated coal chars. Carbon, 2004, 42(12-13), 2451-2455.

[13] Alcañiz-Monge J., Cazorla-Amorós D., Linares-Solano A., Yoshida S., Oya A., Effect of the activating gas on tensile strength and pore structure of pitch-based carbon fibres. Carbon, 1994, 32 (7), 1277-1283.

[14] Mazlana M.A.F., Uemuraa Y., Yusupa S., Elhassana F., Uddin A., Hiwada A., el al., Activated carbon from rubber wood sawdust by carbon dioxide activation. Procedia Eng., 2016, 148, 530-537.

[15] Cheng S., Zhang L.B., Xia H.Y., Peng J.H., Zhang S.Z., Zhou C.J., Preparation of activated carbon from Hawaii nut shell via $CO_2$ activation using response surface methodology. Chin. J. Environ. Eng., 2015, 9(9), 4495-4502.

[16] Luo H.M., Liu J., Feng H.X., Zhang D.Y., Zhang J.Q., Study on activated carbon preparation with abandoned coke fines activated with KOH-$K_2CO_3$. Fuel. Chem. Proc., 2008, 39(4), 42- 45.

[17] Muniandy L., Adam F., Mohamed A.R., Eng-Poh N., The synthesis and characterization of high purity mixed microporous/mesoporous activated carbon from rice husk using chemical activation with NaOH and KOH. Microp. Mesop. Mater., 2014, 197, 316-323.

[18] Xu B., Wu F., Cao G.P., Yang Y.S., Effect of carbonization temperature on microstructure of PAN-based activated carbon fibers prepared by $CO_2$ activation. New Carbon Mater., 2006, 21(1), 14-18.

[19] Huang Y., Huang Y., Wang W.Q., Feng Q.M., Hu S.L., Synthesis and characterization of hydrohar adsorbent from walnut shell. J. Xinjiang Agr. Univ., 2016, 39(2), 149-154.

[20] Liu C.B., Lan X.Z., Tian Y.H., Song Y.H., Influence of carbonization on temperature on the performance of formed activated carbon based on blue-coke. Coal Convers., 2012, 35(2), 69-72.

[21] Jian X.K., Liu S.C., Bian Y., Technique research on preparation of activated carbon from corncob with boric acid catalytic. J. Cent. South. Univ. Forest. Technol., 2012, 32(10), 198-202.

[22] Zhang L.B., Peng J.H., Yang K.B., Xia H.Y., Guo S.H., Zhang S.M., Preparation and characterization of activated carbons from tobacco stems with $CO_2$ activation by microwave irradiation. Chem. Eng., 2007, 35(5), 67-70.

[23] Nabais J.V., Carrott P., Carrott M.R., Luz V., Ortiz A.L., Influence of preparation conditions in the textural and chemical properties of activated carbons from a novel biomass precursor: The coffee endocarp. Bioresource Technol., 2008, 99(15), 7224-7231.

[24] Rodriguez-Reinoso F., Molina-Sabio M., Gonzlez M.T., The use of steam and $CO_2$ as activating agents in the preparation of activated carbons. Carbon, 1995, 33(1), 15-23.

[25] Xing W., Zhang M.J., Yan Z.F., Synthesis and activation mechanism of coke based super activated carbons. Acta. Phys-chim. Sin., 2012, 18(4), 340-345.

[26] Roman S., Gonzalez J.F., Gonzalez C.M., Zamora F., Control of pore development during $CO_2$ and steam activation of olive stone. Fuel Process. Technol., 2008, 89(8), 715-720.